Journal of Engineering and Applied Sciences 13 (Special Issue 14): 11122-11134, 2018
ISSN: 1816-949X
© Medwell Journals, 2018

CFD Analysis for Turbulent Flow and Heat Transfer in U-Tube

[1]Khudheyer S. Mushatet and [2]M. Ayad Ali
[1]Department of Mechanical Engineering, College of Engineering, Thi-Qar University, Al-Nasiriya, Iraq
[2]Al-Mussaib Technical College, Al-Furat Al-Awsat Technical University, Babil, Iraq

Abstract: In this research, three-dimensional incompressible turbulent flow and heat transfer in a circular tube of U-configuration has been investigated numerically. The influences using the U-tube in various downstream lengths and curvature radius ratios on thermal and hydrodynamic fields are presented in details. Two cases for U-tube are tested, the first case is using the tube with different downstream lengths (1, 0.5 and 0.25 m), the second case is using the tube with different curvature radius ratios (1.5, 2 and 2.5).The tube surface is subjected to a constant heat flux and the air is chosen to be the working fluid with turbulent flow under a range of Reynolds number (10000-25000). The turbulent flow and heat transfer is governed by continuity, momentum and energy equations. The effect of turbulence is treated by a k-ε turbulent model. ANSYS Fluent code (15.0) based on finite volume method is used to get the numerical results. The obtained results of increasing the downstream length and reducing the curvature radius ratio showed an increasing in both Nusselt number and friction factor as compared with those of straight tube, for all the considered values of Reynolds number. It is discovered that increasing the downstream length by 50% enhance considerably the heat transfer by about 1.7% and reducing the curvature radius ratio by 100% enhance the heat transfer by about 1.5%, due to the strong intensification of the secondary transverse flows. The maximum enhancement efficiency is obtained for the circular cross-section U-tube with the highest downstream length and lowest curvature radius ratio at Re = 20000. Numerical investigations indicated that within the U-bend, secondary flows partially invert temperature profiles resulting in a significant localized decrease in average fluid temperature at the pipe surface. As a result, a significant heat transfer enhancement is observed. The present numerical results are compared with empirical correlations and verified a comparatively good agreement.

Key words: Turbulent, heat transfer, U-tube, numerical investigation, curvature radius ratio, downstream length

INTRODUCTION

U-tubes (two lengths of straight tube joined by 180° bend at one end) are commonly used in large engineering application, such as heat exchangers, gas turbine blades, waste heat reboilers, nuclear reactors, evaporators and steam generators, e.g., when a fluid moves through a straight tube, the fluid velocity near the centerline is higher than that near the wall. The effect is especially pronounced in laminar flow but is true for turbulent flow, too. When the tube is coiled or bent 180°, all fluid elements experience a centrifugal force radially outward which is proportional to the square of the element velocity and inversely proportional to the radius of the curvature. Therefore, the more rapidly moving elements near the centerline tend to move towards the outside, displacing the slower elements which in turn move back toward the bend axis. The effect is to superimpose a "Secondary" flow pattern upon the primary flow.

Due to the existence of the secondary flow, the heat transfer is higher in a curved tube than in an equivalent straight tube under similar fluid flow conditions and the heat transfer mechanism is more complicated that's the reason of using numerical investigation (Moshfeghian, 1978).

In the tube bend, due to local imbalance among pressure gradient and inertial forces, the flow is characterized as a secondary flow/circulation. It is mainly depend up on the curvature of the pipe which is being a characteristic length of tube cross-section, for instance the radius or hydraulic radius and the radius of curvature.

The characteristics of the secondary flow/ circulation depend not only on Reynolds number and diameter but also on the shape and size of the tube's cross-section. In developing flows, e.g. in the entrance region between a straight tube and a bend, they depend also on the distance from the curve entry.

Corresponding Author: M. Ayad Ali, Al-Mussaib Technical College, Al-Furat Al-Awsat Technical University, Babil, Iraq

The study of turbulent flow and fluid behavior in U-tube configurations has been a subject of interest among many researches. Several researchers have examined the fluid flow and heat transfer characteristics experimentally as well as computationally.

Moshfeghian (1975) heat transfer through a 180 bend tube was studied. A Reynolds range from 7,300-27,000 was investigated for a bend radius of 9.875 inches and 7/8-inch OD (0.052 inch wall thickness). The test section was heated electrically. Analysis of the experimental data obtained in this investigation of the 180 bend indicates that the local heat transfer coefficient in the straight section upstream of the bend is independent of peripheral position. The peripheral heat transfer is far from uniform in the bend, being much higher at the outside and lower at the inside of the bend, resulting in a higher mean heat transfer coefficient as compared to a straight tube under similar conditions. At any cross section in the bend, the distribution of peripheral heat transfer coefficient is almost symmetrical about a plane containing the longitudinal axis of tube and the radius of the bend. At the entrance region of the downstream section of the bend, the distribution of peripheral heat transfer coefficient is symmetrical about the plane of the bend. Also, the peripheral heat transfer coefficient is highest at the outside wall of the bend and lowest at the inside wall. Rowe (1970) experimentally examined the heat transfer effect in large wavy pipe due to secondary flow which leads to complete interchange of fluid in the wall and the central core line. Their research particularly focused on single phase flow in various pipe bends like 180 U-bend, 45°/45° S-bend attached to the end of a long straight pipe. In a 180 bend it is found that, from the start of the bend, the secondary flows increase to a maximum and then decrease to a steady value. This effect is explained by relating the local total pressure gradient to the production of streamwise vortices. Patel and Parekh (2015) carried out the design of optimum size and the temperature difference of U-type shell and tube heat exchanger, general design consideration and design procedure is also illustrated. Different types of methods are carried out for optimum design, by LMTD method, Є-NTU method, P-NTU method and also for Ψ-NTU method, also, according to design parameters experimental analysis is carried out. The results show that keeping the hot water mass flow rate constant at 0.401kg/sec and varying cold water mass flow rate at 0.4785, 0.5173 and 0.5595 kg/sec with increase in cold water temperature of 6.8, 5.7 and 4.9°C, respectively. Based on the design methodology we design and fabricate the shell and U tube heat exchanger and perform the experimental test. Sudo *et al*. (2000) an experimental steady, developing turbulent flow in a circular sectioned 180° bend has been investigated. The bend had a radius of 104 mm and a curvature radius ratio of 4.0 with long, straight upstream and downstream pipes. It was shown that in the section upstream from a bend angle of about 60, both the flows through the 180° and the 90° bend are closely similar in their behavior. In the section from the bend angle of 90°, the high-velocity regions occurred near the upper and lower walls as a result of strong secondary flow and the turbulence with high level emerges in the central region of the bend. Just behind the bend exit, an additional pair of vortices appears in the outer part of the cross section owing to the transverse pressure difference. In the downstream tangent, the flow returns slowly to the proper flow in a straight pipe but it needs a longer distance for recovery than in the 90° bend. Nayak *et al*. (2017) numerically examined the flow and heat transfer characteristics in 180 bend pipe having flow of water-fly ash slurry. In their work they considered RNG k-ε turbulence model. The pressure drop and heat transfer examined for multiphase flow using finite volume approach. The results indicated that for pipe bend the heat transfer coefficient for smaller radius ratio is 53.28% more than the larger radius ratio for the solid concentration of 10% and velocity of 1 m/sec, also the value of the heat transfer coefficient increases with increase in the particle concentration and velocity due to the presence of a secondary flow in the bends. Janyanti *et al*. (1993) performed CFD analysis to examine the Gas-particle motion in 90 and 180° circular cross-section pipe bends. They found that the secondary flow induced in the gas phase due to curvature affects the motion of the particles which causes the smaller particles to come out of the bend without deposition. Munch and Metais (2007) investigated numerically the influence of the curvature radius "Rc" on the flow carrying out three Large Eddy Simulations (LES) for U-bends with Rc/D_h = 3.5, 6.5 and 10.5. It's observed that the decrease of the curvature Radius was accompanied by a strong intensification of the secondary transverse flows. They also showed that the secondary flows strength was directly related to the radial pressure gradient intensity. Clarke and Finn (2008) studied the enhancement of internal convection heat transfer following a heat exchanger U-bend under laminar flow conditions. Numerical investigations, conducted using "Fluent" computational fluid dynamics, to investigate the development of temperature profiles upstream of within and downstream of a U-bend for a laminar flow refrigerant.

The model geometry utilized in this study consisted of a U-bend preceded by a straight circular inlet pipe and followed by an identical straight circular outlet pipe. It was shown that centrifugally induced secondary flows, known as dean vortices, partially invert the temperature profile. It was found that Nusselt values downstream of a U-bend were found to exceed Nu values for a combined entry situation by >20% for up to 20 pipe diameters downstream. Azzola *et al.* (1986) used laser-Doppler velocimetry measurement to examine the turbulent flow in a 180 pipe bend. Numerical simulations have reproduced with a gratifying degree of fidelity the measured evolution of the flow. Predictions of the flow development were presented based on a "semielliptic" truncation of the Reynolds equations in the main part of the flow with the standard k-ε effective viscosity model used to approximate the turbulent stress field. They found that the bend of angle between 90 and X/D = 5 (X and D being the axial distance from the pipe inlet and pipe diameter, respectively), the circumferential velocity profiles displayed secondary flow reversals which are independent of the Reynolds number.

The present investigation is undertaken to study the effect of a 180° bend on heat transfer to a single phase fluid in tubes and to obtain a better and more quantitative insight into the heat transfer process that occurs when a fluid flows in a U-bend tube, so, the objectives of this steady can be abbreviated as follows:

- Investigate the hydrodynamics and thermal performance of U-shaped tube as compared with straight one
- Assessment the variation in curvature radius ratio and downstream length on heat transfer enhancement and overall performance

MATERIALS AND METHODS

Model description: The physical domain consist of U-tube configuration, this configuration consists of three parts, i.e., the upstream tube, the U-bend and the downstream tube. Three cases for U-tube geometry are investigated as follows:

Case 1: The configuration consists of a circular cross-sectional tube, the length of the upstream tube is 20 times the diameter of the tube while the length of the downstream tube L_{DS} is 5, 10 and 20 times the diameter of the tube which is (1, 0.5 and 0.25 m). The curvature Radius ratio "Rc" equal to 1.5 as shown in Fig. 1.

Case 2: The configuration consists of circular U-tube with different values of dimensionless parameter called curvature Radius ratio "Rc". Three different bends have been studied depending on "Rc" (that is equal to the radius of the U-bend curvature to the hydraulic diameter of the tube, $Rc = R/D_h$) which is (1.5, 2 and 2.5) as shown in Fig. 2.

Air flows in the tube, enters with a different velocities and the outlet is assumed to be an outflow boundary. Turbulent, isothermal and steady state conditions will be considered to solve the flow field. The study has covered four Reynolds numbers from 10000-25000 and a constant Prandtl number. Local heat transfer coefficients were computed from knowledge of local heat flux values along the test section which is 1000 w/m^2.

Mathematical model and numerical analysis

Assumptions: The following assumptions are used to simplify the proposed model solution:

- The fluid is air
- The fluid has constant properties
- Steady state flow
- Incompressible flow
- The gravity effect is neglected
- Non-slip flow is assumed
- The dissipation of heat is assumed to be neglected
- Negligible wall thickness

Governing equations for the turbulent flow: The description of the fluid motion in the tube for the turbulent state is made by solving the average differential equation of mass (continuity) and momentum equation in addition to the (k-ε) Model equation. The turbulent flow is characterized by fluctuation velocity field.

In describing the turbulence flow in mathematical terms, it's convenient to separate it into mean motion and a fluctuation or eddy motion. As in the following form:

Continuity equation:

$$\frac{\partial u}{\partial x}\frac{\partial v}{\partial y}\frac{\partial w}{\partial z}0 \quad (1)$$

Continuity equation is a mathematical representation for the mass conservation. Its form is (Kumar, 2010).

Momentum equations (NSEs): Momentum equation in x-direction:

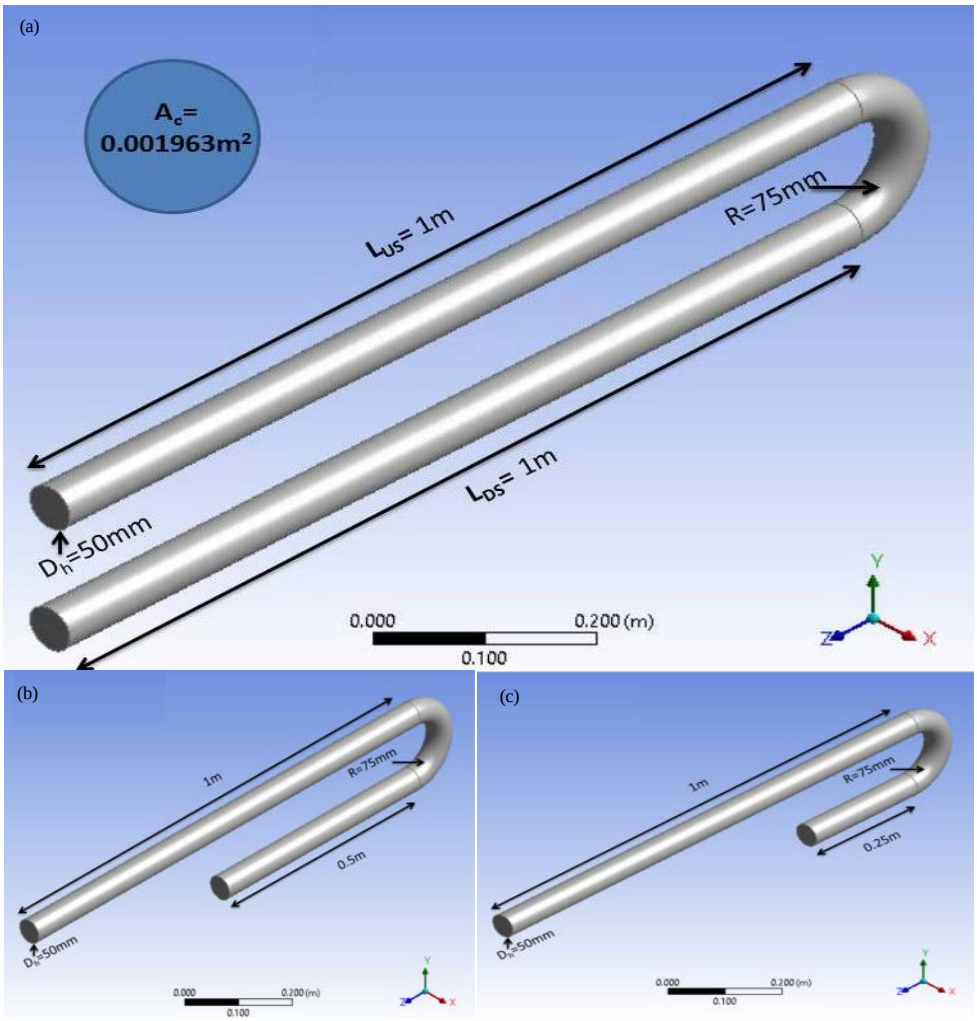

Fig. 1: The geometry of the U-bend tube with different downstream length (a-c is L_{DS} = 1, 0.5 and 0.25 m)

$$\rho\left(\frac{\partial u^2}{\partial x}+\frac{\partial uv}{\partial y}+\frac{\partial uw}{\partial z}\right)=-\frac{\partial p}{\partial x}+\frac{\partial}{\partial x}\left(2\mu_{eff}\frac{\partial u}{\partial x}\right)+\frac{\partial}{\partial y}\left(\mu_{eff}\frac{\partial u}{\partial y}\right)+\frac{\partial}{\partial z}\left(\mu_{eff}\frac{\partial u}{\partial z}\right)\frac{\partial}{\partial y}\left(\mu_{eff}\frac{\partial v}{\partial x}\right)\frac{\partial}{\partial z}\left(\mu_{eff}\frac{\partial w}{\partial x}\right) \quad (2)$$

Momentum equation in y-direction:

$$\rho\left(\frac{\partial vu}{\partial x}+\frac{\partial v^2}{\partial y}+\frac{\partial vw}{\partial z}\right)=-\frac{\partial p}{\partial y}+\frac{\partial}{\partial x}\left(\mu_{eff}\frac{\partial v}{\partial x}\right)+\frac{\partial}{\partial y}\left(2\mu_{eff}\frac{\partial v}{\partial y}\right)+\frac{\partial}{\partial z}\left(\mu_{eff}\frac{\partial v}{\partial z}\right)+\frac{\partial}{\partial x}\left(\mu_{eff}\frac{\partial u}{\partial y}\right)+\frac{\partial}{\partial z}\left(\mu_{eff}\frac{\partial w}{\partial y}\right) \quad (3)$$

Momentum equation in z-direction:

$$\rho\left(\frac{\partial wu}{\partial x}+\frac{\partial wv}{\partial y}+\frac{\partial w^2}{\partial z}\right)=-\frac{\partial p}{\partial z}+\frac{\partial}{\partial x}\left(\mu_{eff}\frac{\partial w}{\partial x}\right)+\frac{\partial}{\partial y}\left(\mu_{eff}\frac{\partial w}{\partial y}\right)+\frac{\partial}{\partial z}\left(2\mu_{eff}\frac{\partial w}{\partial z}\right)+\frac{\partial}{\partial x}\left(\mu_{eff}\frac{\partial u}{\partial z}\right)+\frac{\partial}{\partial y}\left(\mu_{eff}\frac{\partial v}{\partial z}\right) \quad (4)$$

where, μ_t is the eddy or turbulent, viscosity. In turbulent flow governing Eq. 4-6, the terms of turbulent stresses are added to the terms of laminar stresses using the concept of effective viscosity:

$$\mu_{eff}=\mu+\mu_t \quad (5)$$

Energy equation:

$$\frac{\partial uT}{\partial x}+\frac{\partial vT}{\partial y}+\frac{\partial wT}{\partial z}=\frac{\partial}{\partial x}\left(\Gamma_{eff}\frac{\partial T}{\partial x}\right)+\frac{\partial}{\partial y}\left(\Gamma_{eff}\frac{\partial T}{\partial y}\right)+\frac{\partial}{\partial z}\left(\Gamma_{eff}\frac{\partial T}{\partial z}\right) \quad (6)$$

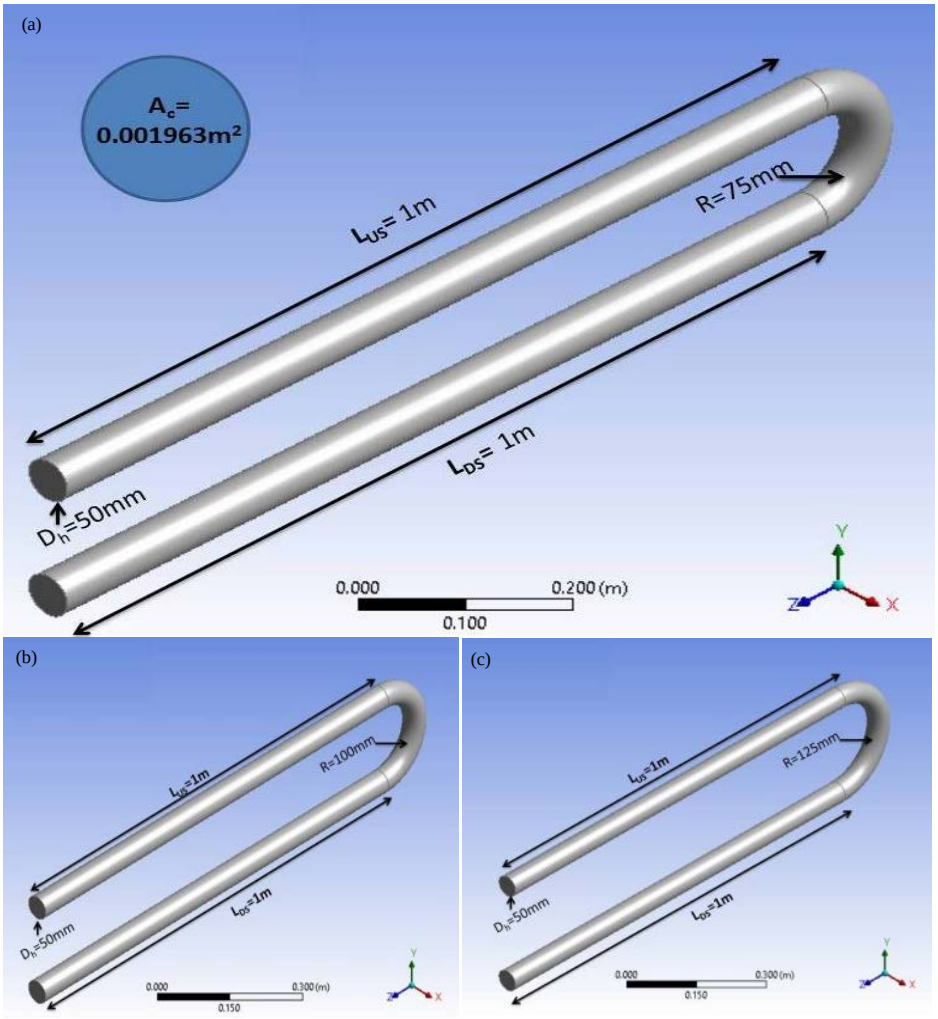

Fig. 2: The geometry of the U-bend tube with different curvature radius ratio (a-c is Rc = 1.5, 2, 2.5)

The standard k-ε Model: The standard k-ε Model has two model equations one for k and one for ε. The model transport equation for k is derived from the exact equation while the model transports equation for ε was obtained by using the physical analysis. The standard model uses the following transport equations for k and ε. For turbulent kinetic energy (k):

$$\rho\left(\frac{\partial}{\partial x}(ku)+\frac{\partial}{\partial y}(kv)+\frac{\partial}{\partial z}(kw)\right)=\frac{\partial}{\partial x}\left(\frac{\mu_t}{\sigma_k}\frac{\partial k}{\partial x}\right)+\frac{\partial}{\partial y}\left(\frac{\mu_t}{\sigma_k}\frac{\partial k}{\partial y}\right)+\frac{\partial}{\partial z}\left(\frac{\mu_t}{\sigma_k}\frac{\partial k}{\partial z}\right)+G-\rho \quad (7)$$

For energy dissipation rate (ε):

$$\rho\left(\frac{\partial}{\partial x}(u)+\frac{\partial}{\partial y}(v)+\frac{\partial}{\partial z}(w)\right)=\frac{\partial}{\partial x}\left(\frac{\mu_t}{\sigma_\varepsilon}\frac{\partial}{\partial x}\right)+\frac{\partial}{\partial y}\left(\frac{\mu_t}{\sigma_\varepsilon}\frac{\partial}{\partial y}\right)+\frac{\partial}{\partial z}\left(\frac{\mu_t}{\sigma_\varepsilon}\frac{\partial}{\partial z}\right)+C_1\rho\frac{\varepsilon}{k}G-C_2\rho\frac{\varepsilon^2}{k} \quad (8)$$

where, G is referred to the generation term and is given (Al-Aboodi, 2010):

$$G=\mu_t\left[2\left(\frac{\partial u}{\partial x}\right)^2+2\left(\frac{\partial v}{\partial y}\right)^2+2\left(\frac{\partial w}{\partial z}\right)^2+\left(\frac{\partial v}{\partial y}\frac{\partial u}{\partial x}\right)^2+\left(\frac{\partial v}{\partial z}\frac{\partial w}{\partial x}\right)^2+\left(\frac{\partial v}{\partial z}\frac{\partial w}{\partial y}\right)^2\right] \quad (9)$$

Also:

$$k=1/2(\overline{u'^2}+\overline{v'^2}+\overline{w'^2}) \quad (10)$$

$$\varepsilon = \overline{e_{ij}' \square e_{ij}'} \quad (11)$$

The turbulent kinetic energy (k) and the dissipation rate of the turbulent kinetic energy (ε) are chosen as the two properties to determine the turbulent viscosity. Where:

$$\mu_t = \rho c_\mu \frac{k^2}{\varepsilon} \quad (12)$$

where, c_μ is a constant.

Boundary conditions: The boundary conditions are specified for each zone of the computational domain as follow:

Inlet boundary conditions:

- Uniform inlet velocity, $U = U_{in}$
- The flow is isothermal ($T = T_{in} = 300$ K)

Wall boundary condition:

- The velocity at the walls is taken to be zero (no slip). ($u = v = w = 0$) in the x, y and z direction
- A constant heat flux ($q = 1000 W/m^2$) concentrated on the whole surface area of the wall in the circular cross-section tube

Outlet boundary condition: Zero gage pressure is specified at the outlet domain.

Hydrodynamic parameters: In this study, signification parameters are defined as: The Reynolds number is defined by Eq. 13-14:
Re = Inertial forces/viscous forces:

$$Re = \rho U_{in} D_h / \mu \quad (13)$$

where, D_h is the hydraulic diameter:

$$D_h = \frac{4A_{sec}}{P_{er}} \quad (14)$$

Friction coefficient: The friction coefficient can be expressed in shear stress at the channel surface is defined as:

$$C_f = \tau_w \frac{1}{2} \rho U^2 \quad (15)$$

where, τ_w is the wall shear stress and defined as:

$$\tau_w = \mu \sqrt{(\frac{\partial u}{\partial y})^2 + (\frac{\partial w}{\partial y})^2} \quad (16)$$

For the turbulent flow and due to complex behave of this flow the friction factor always calculates from the experimental equations. Therefore, for the turbulent flow $Re \leq 2 \times 10^4$ friction factor is given by Saysroy and Eiamsa-ard (2017):

$$f = 0.316 Re_{D_h}^{-1/4} \quad (17)$$

In addition, friction coefficient (Fanning fraction factor) is given by:

$$c_f = \frac{f}{4} \quad (18)$$

The bulk temperature; The bulk temperature is described as:

$$T_b = \frac{\int T_i \rho dV_i}{\int \rho dV_i} = \frac{\sum_{i=1}^{n} T_i \rho |V_i|}{\sum_{i=1}^{n} \rho |V_i|} \quad (19)$$

The wall temperature: the wall temperature is described as:

$$T_w = \frac{1}{A} \int T_i \, dA_i = \frac{1}{A} \sum_{i=1}^{n} T_i |A_i| \quad (20)$$

The pressure drop was calculated by surface integral by means of area weighted average:

$$P = \frac{1}{A} \int P dA \quad (21)$$

The coefficient of heat transfer is defined as:

$$h = \frac{q''}{Tw\text{-}Tb} \quad (22)$$

where, q" is the heat flux. The Nusselt number: the Nusselt number is defined as:

$$Nu \frac{h . D_h}{K} \quad (23)$$

The Radius curvature ratio (Rc):

$$Rc = R/D_h \quad (24)$$

where, R is the tube curvature Radius.

Numerical analysis: Computational Fluid Dynamics (CFD) is considered the science that helps the computers

Table 1: Different grids and their Nusselt number and friction factor results for different studied cases

Cases/No. of grid elements	Nu	$Nu_{deviation}$	f	$f_{deviation}$
ST				
465,094	37.1807	0.017957	0.033993	0.023358
541,082	37.86056	0.044694	0.034806	0.042845
683,636	39.63186		0.036364	
CUT				
1,008,000	40.05469	0.011956	0.037385	0.028532
1,197,774	40.53936	0.021926	0.038483	0.025722
1,480,347	41.44816		0.039499	
CUT with LDS = 0.5 m				
758,784	39.35966	0.03254	0.037079	0.034753
970,776	40.6835	0.005527	0.038414	0.019876
1,047,600	40.90960		0.039193	
CUT with LDS = 0.25 m				
638,510	39.1067	0.01517	0.037002	0.020308
712,050	39.70907	0.012275	0.037769	0.011412
829,578	40.20254		0.038205	
CUT with Rc = 2				
959,889	39.2036	0.027685	0.036857	0.024353
1,049,622	40.31984	0.002167	0.037777	0.011177
1,237,194	40.4074		0.038204	
CUT with Rc = 2.5				
1,191,095	39.16034	0.035202	0.036816	0.035599
1,273,857	40.58917	0.01863	0.038175	0.01659
1,336,384	41.35972		0.038819	

to produce quantitative calculation of fluid flow basis. This includes the governing fluid motion and conservation laws and considered the tools basis to design and develops the engineering application. CFD is become necessary work of many researchers in the world because it used predict internal flow and the development of computer became accurate and near to the fact. Fluent program is used in advanced numerical applications to solve many problems in order to achieve effective results for many different models.

Grid independency: A grid independence study is made to choose the optimum grid to get a better solution. The present results consider three different values for the grid independency investigate. The results are summarized in Table 1 shows the specified grid for all shapes. The Nusselt number is determined for all shapes at Re = 10000. It is found that there is a small change in the average value of Nusselt number. The grid resolution investigation reveal that ST, CUT, CUT(L_{DS} = 0.5 m), CUT (L_{DS} = 0.25 m), CUT (Rc = 2) and CUT (Rc = 2.5) become independent of the grid at cells 541,082, 1,197,774, 1,047,600, 829,578, 1,237,194 and 1,336,384 cells respectively.

Solving by Fluent: The numerical method of discredited governing equations can be solved by writing a code or the problem can be solved by using one of the commercial (CFD) code. ANSYS Fluent 15.0 Software is used to calculate the current numerical investigation, since, Fluent is generally used in this field and it is considered one of the greater among other available codes. With a RNG (k-ε) Model, a finite volume discretization is used in approximating the governing equations. A double-precision and pressure-based solver is used in the numerical computation. A non-slip boundary condition is adopted on pipe surface. The simple algorithm is used for pressure-velocity coupling. A second-order upwind scheme was adopted to the discretization of all terms.

RESULTS AND DISCUSSION

In this study, the numerical results have been addressed to verify the intensification of forced convection in a U-tube configuration with different shapes. The hydraulic diameter of the U-tubes is (0.05 m). Two cases for U-tube are discussed, the first case is a circular cross section U-tube with different downstream length (1, 0.5 and 0.25 m) and compare the result with a Straight Tube (ST) of the same cross sectional area and a length of (1 m), the second case is circular cross section U-tube with a different curvature Radius ratio "Rc" (1.5, 2, 2.5) and compare the result with the straight tube.

Case 1 (Effect of downstream length): The effect of the downstream length on the average Nusselt number variation for different values of Reynolds number is described in Fig. 3. It is observed that the Nusselt number increases as the downstream length increases for all the considered values of Reynolds number. However, this increase seems to larger for high Reynolds number (Re = 15000-20000). The highest downstream length (L_{DS} = 1 m) indicated the maximum increase in Nusselt number as compared with other downstream lengths. The results verified that the enhancement in the mean Nusselt is found to be 8.6, 7 and 5.3% for L_{DS} = 1, 0.5 and 0.25 m, respectively as compared with the straight tube. It can be noted that utilize of the U-bend configuration lead to greater heat transfer for all the considered downstream length values. The cause is attributed to the flow

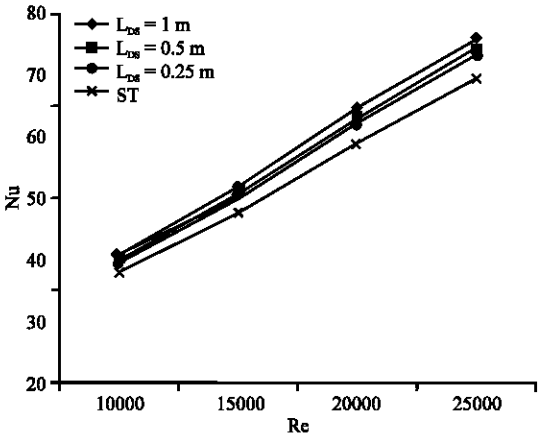

Fig. 3: Effect of downstream length on Nusselt number for circular cross section U-tube

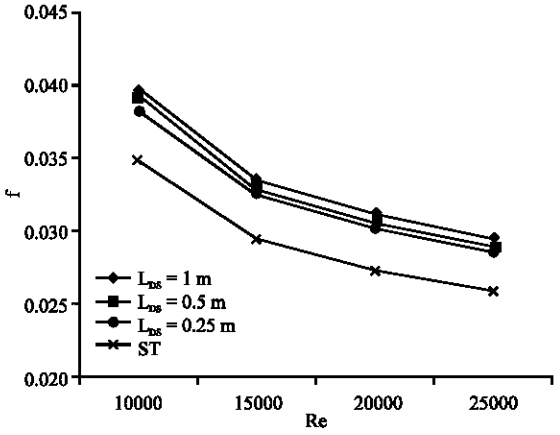

Fig. 4: Effect of downstream length on friction factor variation for circular cross section U-tube

separation and secondary flow formation at the bend section and consequently a superior disorganized mixing between the central and the wall areas. This flow mixing disturbs the boundary layer and as a result intensification the heat transfers.

Figure 4 shows the influence of the downstream length on the average friction factor variation for different values of Reynolds number. It can be noticed that the friction factor acquired from the three various downstream lengths are reduces with intensifying Reynolds number. It is viewed from the figure that there is significant decrease in the friction factor for utilizing L_{DS} = 0.5, 0.25 m and there is a significant rise in the friction factor for the higher downstream length, particularly at L_{DS} = 1 m. The gained results indicated that the increase in the friction factor is found to be 1.95 and 3.3% for L_{DS} = 1 m as compared with the downstream length L_{DS} = 0.5 and 0.25 m. It can be observed that use of the U-bend

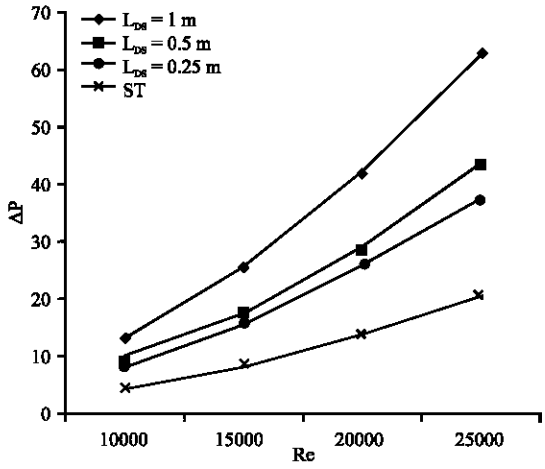

Fig. 5: Effect of downstream length on pressure drop variation for circular cross section U-tube

configuration lead to greater friction factor for all the considered downstream length values. This is because of the wall shear stress at the bend section, i.e., at inner region and at outer region is quite different, the inner region experience higher rate of friction and shear stress as compared to the outer region

The influence of the downstream length on the pressure drop variation for different values of Reynolds number is depicted in Fig. 5. It can be examined that the pressure losses obtained from using three different downstream lengths are increased with the increase of Reynolds number. The highest downstream length (L_{DS} = 1 m) denoted the highest growth in pressure drop as contrasted with other downstream lengths. The collected results illustrated that the rise in the pressure loss is found to be 40.8 and 64.6% for L_{DS} = 1 m as compared with the downstream length L_{DS} = 0.5 and 0.25 m. The rise in pressure loss with U-bend configuration is widely greater contrast than the straight tube, this is because of the dispersion of the dynamic pressure of the fluid due to centrifugal force that drives fluid from the bend outside around the tube wall towards the bend inside, that is produces a reverse flow and due to the length of the U-tube which is greater than of the straight tube.

The temperature variation along the domain is exposed in Fig. 6. This variation in temperature distribution was displayed for the case of circular U-tube and the effect of the downstream length variation for air flowing with Re = 15000.

For an upstream length tube, the fluid temperature reduces radially from the tube wall to its midpoint in a circular model due to the absence of reverse flow. As the fluid flows more downstream, its temperatures will rise

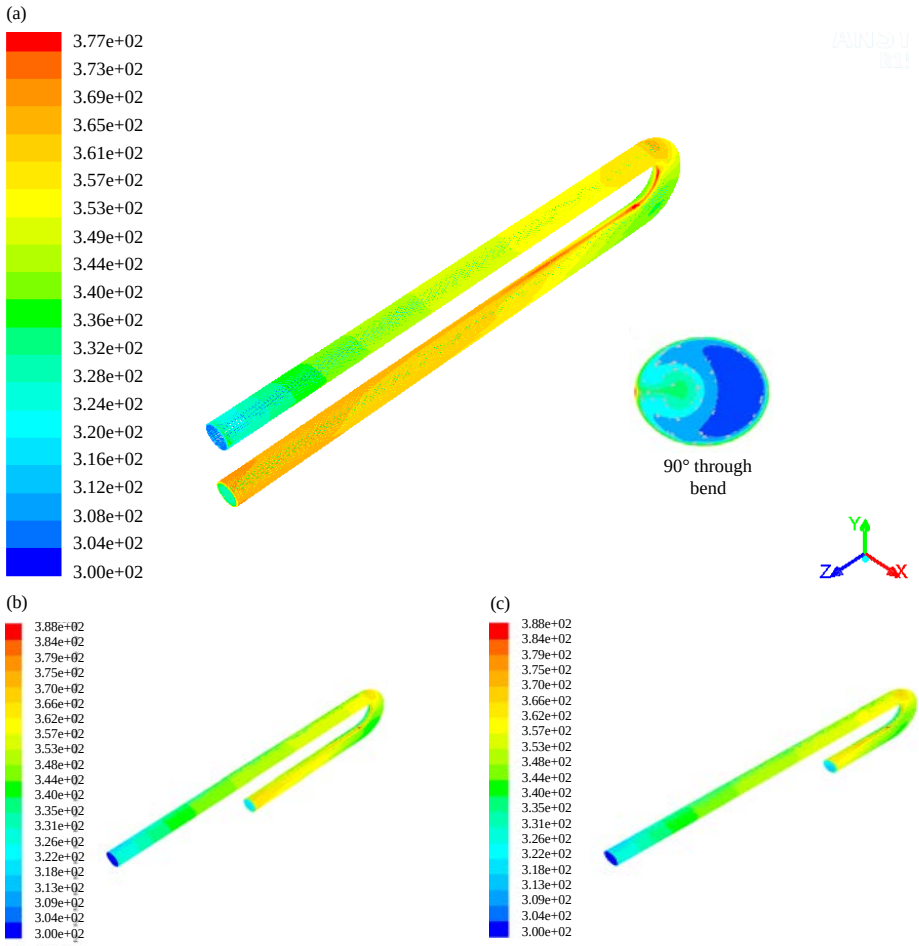

Fig. 6: Temperature-contour for circular U-tube for Re = 15000 of deferent downstream length; a) L_{DS} = 1 m; b) L_{DS} = 0.5 m and c) L_{DS} = 0.25 m

forcing the colder area which lies at the tube center, to be smaller and smaller due to rising in heat attracted by the fluid from the tube wall and the growing of thermal boundary layer. As showed through the figure, when the fluid enters the U-bend area the temperature distribution will disrupt. The secondary flows are observed to drive cold fluid from the core of the tube towards the outside of the tube wall, this cold fluid replaces warm fluid that had developed at the tube walls as the fluid moved through the inlet tube. The warm fluid is simultaneously driven by the secondary flow, around the tube walls towards the bend inside wall and onwards towards the tube core. Consequently, the thermal boundary layer is eliminated and a sudden drop in fluid temperature at the surface of the tube occurs within the bend. This temperature drop and elimination of the thermal boundary layer that causes the subsequent downstream heat transfer enhancement. This figure shows that the using of U-bend configuration will increase the range of temperature gradient when contrasted with that of straight tube. This influence is related to rising in the mixing of the flow.

Case 2 (Effect of curvature radius ratio): The effect of the curvature radius ratio on the average Nusselt number variation for different values of Reynolds number is described in Fig. 7 It is observed that the Nusselt number increases as the curvature radius ratio decrease for all the considered values of Reynolds number which is agreed with Munch and Metais (2007). The lowest curvature radius ratio (Rc = 1.5) indicated the maximum increase in Nusselt number as compared with other downstream length. The results verified that the enhancement in the mean Nusselt is found to be 7.9, 7.4 and 7% for Rc = 1.5, 2 and 2.5, respectively as compared with the straight tube, the decrease of the curvature radius was accompanied by a strong intensification of the secondary transverse flows. It can be noted that using of the U-bend configuration lead to greater heat transfer for all the considered curvature radius ratio values. This is due to the development of secondary flows at the bend section. This flow mixing disturbs the boundary layer and as a result intensification the heat transfers.

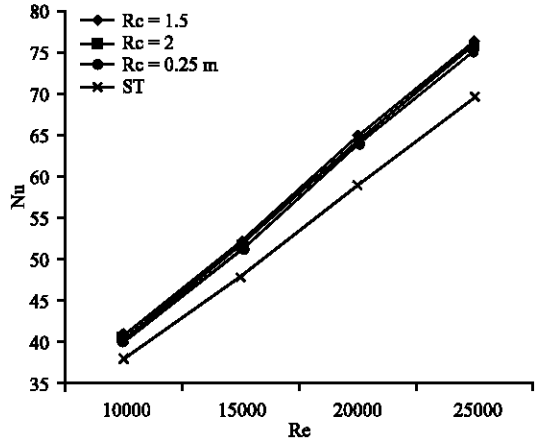

Fig. 7: Effect of curvature radius ratio on Nusselt number for circular cross section U-tube

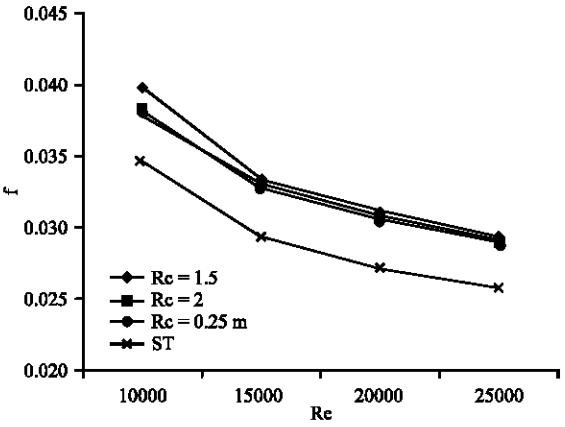

Fig. 8: Effect of curvature radius ratio on friction factor variation for circular cross section U-tube

Figure 8 shows the influence of the curvature radius ratio on the average friction factor variation for different values of Reynolds number. It can be noticed that the friction factor acquired from the three various curvature radius ratios are reduces with intensifying Reynolds number. It is viewed from the figure that there is decrease in the friction factor for utilizing Rc = 2, 2.5 and there is a rise in the friction factor for the lower curvature radius ratio, particularly at Rc = 1.5. The gained results indicated that the increase in the friction factor is found to be 1.8 and 2.4% for Rc = 1.5 as compared with the curvature radius ratio Rc = 2 and 2.5. Decreasing the curvature radius ratio of the bend, causes more enhancement of the secondary flow. The secondary flow results a very high frictional loss in the tube bend compared to straight tubes under similar conditions. It can be observed that use of the U-bend configuration leads to more friction factor for all the considered curvature radius ratio values.

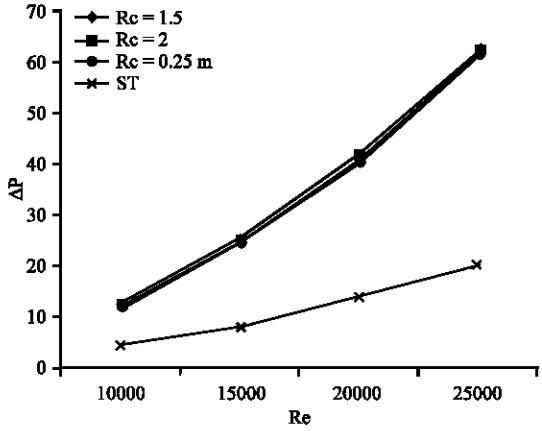

Fig. 9: Effect of curvature radius ratio on pressure drop variation for circular cross section U-tube

The pressure losses suffered in a bend are caused by both friction and momentum exchanges, resulting from a change in the direction of flow. Both these factors depend on the bend angle, the curvature ratio and the Reynolds number.

The influence of the curvature radius ratio on the pressure drop variation for different values of Reynolds number is shown in Fig. 9. It can be examined that the pressure losses obtained from using three different curvature radius ratios are increased with the increase of Reynolds number. The lowest curvature radius ratio (Rc = 1.5) denoted the highest growth in pressure drop as contrasted with other curvature radius ratios. The collected results illustrated that the rise in the pressure loss for Rc = 1.5 as compared with the curvature radius ratios Rc = 2 and 2.5 is 1.8 and 4.2%, respectively. The rise in pressure loss with U-bend configuration is greater than the straight tube, this is due to the centrifugal force that drive the fluid from the bend outside around the tube wall towards the bend inside, In addition to the transverse velocity components of a secondary flow in the bends.

The temperature variation along the domain is exposed in Fig. 10. This variation in temperature distribution was displayed for the case of circular U-tube and the effect of the curvature radius ratio variation, for air flowing with Re = 15000.

For an upstream length tube, the fluid temperature reduces radially from the tube wall to its midpoint in a circular model. As the fluid flows more downstream, its temperatures will rise forcing the colder area which lies at the tube center. As showed through the Fig. 10, when the fluid enters the U-bend area the temperature distribution will disrupt and thermal boundary layer is eliminated and a sudden drop in fluid temperature at the surface of the tube occurs within the bend. Due to the high circulation

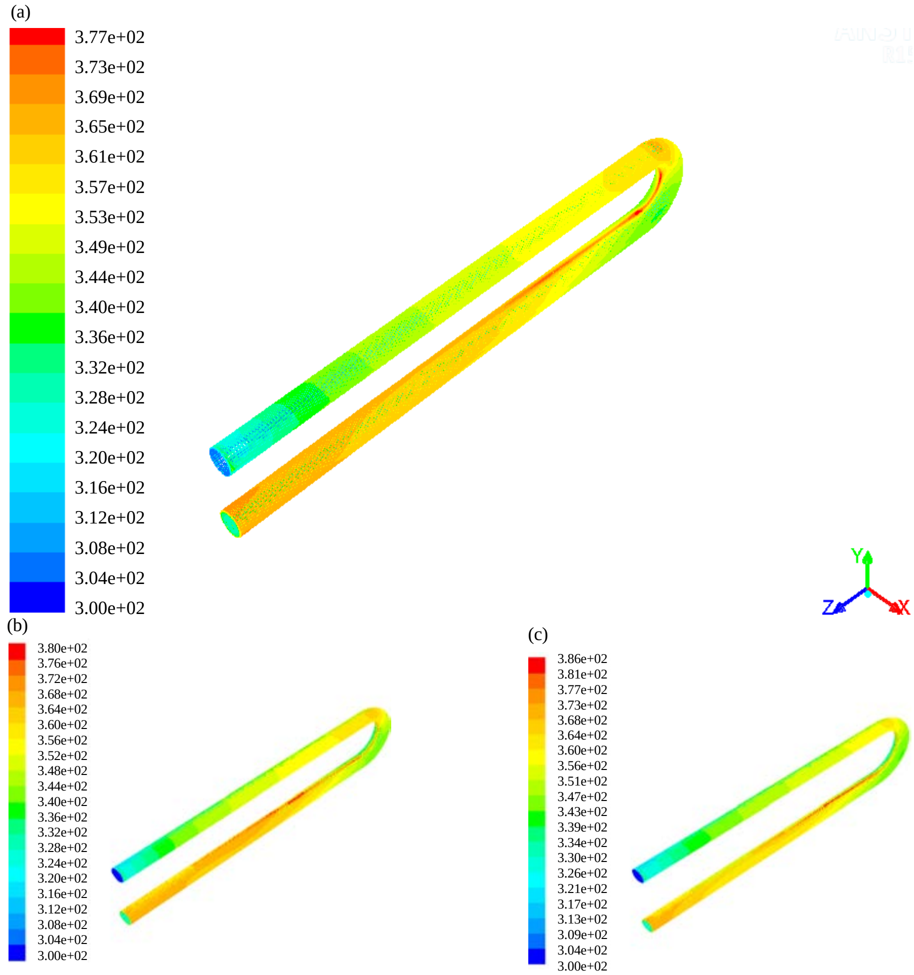

Fig. 10: Temperature-contour for circular U-tube forRe = 15000 of different curvature radius ratio; a) Rc = 1.5; b) Rc = 2 and c) Rc = 2.5

when the radius curvature ratio decreases the temperature reduces in the U-bend and growth take place in heat transfer enhancement. This figure shows that the using of U-bend configuration will increase the range of temperature gradient when contrasted with that of straight tube.

The comparison between the numerical work and published results: The collected numerical results are validated with existing empirical correlations for Nusselt number and friction factor. Before the primary analysis, Nusselt numbers for the U-tube are calculated under a consistent heat flux condition and then contrasted with those acquired from the essential Eq. 25 by Dittus and Boelter:

$$\text{Nu} = 0:023\text{Re}^{0.8}\,\text{pr}^{0.4} \quad (25)$$

Figure 11 exposes that the heat transfer results of the present work agree appropriately with those acquired from

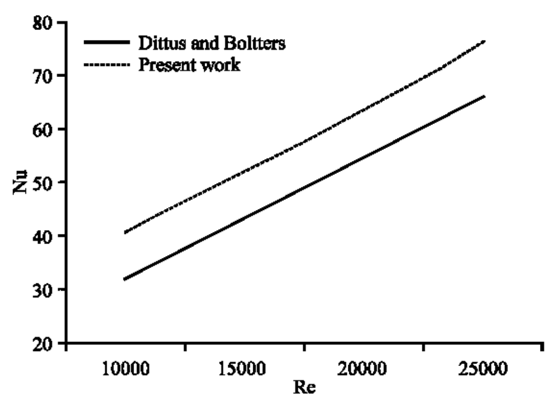

Fig. 11: Validation the present results of average Nusselt number with Dittus and Boltters

Eq. 25 with the differences of less than ±21.7%. The variations of friction factor with Reynolds number for the existing plain tube are offered in Fig. 12. It is

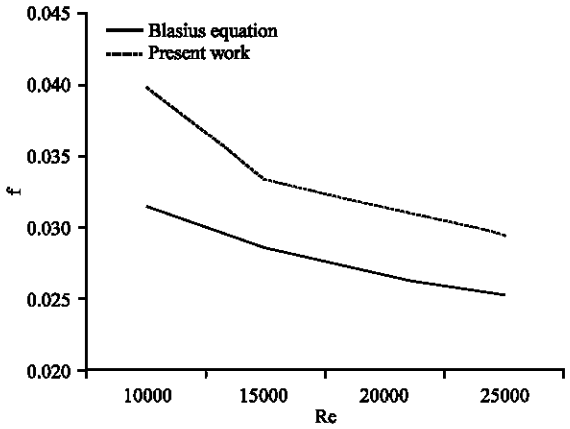

Fig. 12: Validation the present results of average friction factor with Blasius

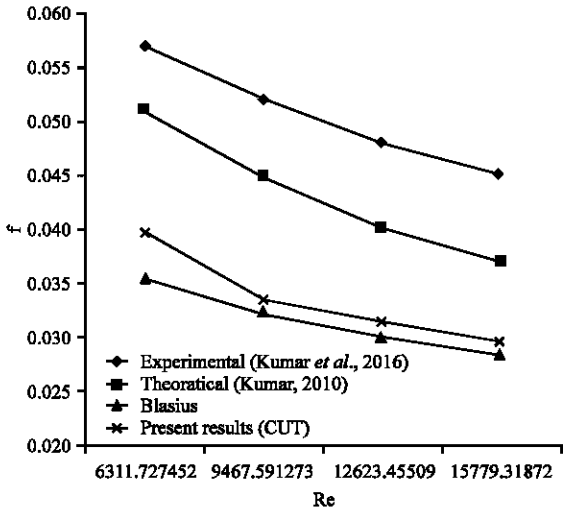

Fig. 13: Validation of the theoretical works with results of (Kumar *et al.*, 2016) and Blasius equation for circular cross section U-tube

realized that the friction factors are within ±20% as contrasted to those accomplished from Blasius correlation:

$$f = 0.316\,Re^{-0.25} \quad (26)$$

Validations: The results of friction factor for U-tube found through this work numerically for the experimental works by Kumar *et al.* (2016). The validations includes the friction factor as displayed in Fig 13. The average deviation for average friction factor between the experimental works by Kumar *et al.* (2016) and the theoretical works is 14% and between the Blasius equation for Kumar *et al.* (2016) and the theoretical works is 27%.

CONCLUSION

The heat transfer intensification in a heated U-tube with different configurations has been numerically investigated. In this study, the following conclusions can be collected. The heat transfer in the tube could be augmented highly by using U-bend configuration. On comparing the performance in terms of heat transfer between straight tube and U-bend tube, U-bend tube yields better performance and heat transfer. The higher downstream length and lower curvature radius ratios of the U-tube accomplish better intensification of heat transfer rate and enhancement efficiency for all cases. The enhancement efficiency for a circular cross-section U-tube, with higher downstream length and lower curvature radius ratio is found to be higher as compared with all other cases. The optimum enhancement efficiency is ranged between 1.07-1.099 for using the circular cross-section U-tube with Rc = 1.5 and L_{DS} =1 m. Heat transfer coefficient and friction factor increases with the decrease in curvature radius ratio and increase the downstream length as compared with the straight tube. The Nusselt number increases with reduction of the curvature radius ratio and increasing Reynolds number. The maximum heat transfer rates is obtained from using the circular cross-section U-tube with Rc = 1.5. Empirical relations for the Nusselt number and friction factor are presented for a comparison use. The enhancement in the mean Nusselt for utilizing the different downstream lengths is found to be 8.6, 6.7 and 5.1% for L_{DS} = 1, 0.5 and 0.25 m, respectively as compared with the straight tube. The enhancement in the mean Nusselt for utilizing the different curvature radius ratios is found to be 8.6, 8.08 and 7.59 % for Rc = 1.5, 2 and 2.5, respectively as compared with the straight tube. Friction factor reduces with rising Reynolds number for various U-tubes with different configurations. As curvature radius ratio increases friction factor reduces. The pressure drop at the bend section, is quite complex as compared to straight pipe. All U-tube configurations provide a considerable increase in pressure drop over the straight tube. The increase in the pressure drop of the CUT with L_{SD} = 1 m is found to be 28.9 and 39.2% over that for using L_{SD} of (0.5 and 0.25 m), respectively and about 66.8% over the straight tube. The average wall temperature for utilizing the circular cross-section U-tube are observed to be proportional directly to the downstream length and inversely to the curvature radius ratio, for the same cross-sectional area. The increase in the pressure drop for the U-tube with Rc = 1.5 is found to be 1.76 and 4.02% over that for using Rc of (2 and 2.5), respectively and to be about 66.8% over the straight tube. The fluid

circulation in the U-bend area for employing the circular cross-section are observed to be proportional inversely to the downstream length and the curvature radius ratio on Reynolds number equal to 15000.

REFERENCES

AL-Aboodi, H.M.A., 2010. Three-dimensional numerical study of laminar and turbulent flow in sudden expansion channel. MSc Thesis, University of Basrah, Basrah, Iraq.

Azzola, J., J.A.C. Humphrey, H. Iacovides and B.E. Launder, 1986. Developing turbulent flow in a U-bend of circular cross-section: Measurement and computation. J. Fluids Eng., 108: 214-221.

Clarke, R. and D. Finn, 2008. Numerical investigation of the influence of heat exchanger U-bends on temperature profile and heat transfer of secondary working fluids. Proceedings of the 5th International Conference on European Thermal-Sciences, May 18-22, 2008, UCD Institute for Discovery, Eindhoven, Netherlands, pp: 1-9.

Jayanti, S., G.F. Hewitt, M.J. Mohideen and M.J. Wang, 1993. Gas-particle flow through bends. Inst. Mech. Eng. Conf. Publ., 5: 161-166.

Kumar, K.L., 2010. Engineering Fluid Mechanics. 7th Edn., S. Chand Group, New Delh, India, ISBN:13-9788121901000, Pages: 611.

Kumar, M., V.K. Yadav, B. Verma and K.K. Srivastava, 2016. Experimental study of friction factor during convective heat transfer in miniature double tube Hair-pin heat exchanger. Proc. Technol., 24: 669-676.

Mahdi, H., 2004. Numerical and experimental study of enhancement of heat transfer in roughened ribbed duct. PhD Thesis, Department of technical Eduction, University of technology, Baghdad, Iraq.

Moshfeghian, M., 1975. The effect of a 180° bend on turbulent heat transfer coefficient in a pipe. PhD Thesis, Oklahoma State University, Stillwater, Oklahoma.

Moshfeghian, M., 1978. Fluid flow and heat transfer in U-bends. Ph.D Thesis, Oklahoma State University, Stillwater, Oklahoma.

Munch, C. and O. Metais, 2007. Large eddy simulations in curved square ducts: Variation of the curvature radius. J. Turbul., 8: 1-18.

Nayak, B.B., D. Chatterjee and A.N. Mullick, 2017. Numerical prediction of flow and heat transfer characteristics of water-fly ash slurry in a 1800 return pipe bend. Intl. J. Therm. Sci., 113: 100-115.

Patel, D.B. and J.R. Parekh, 2015. Design and experimental analysis of shell and tube heat exchanger (U-Tube). Intl. J. Adv. Res. Eng. Sci. Manage., 1: 1-8.

Rowe, M., 1970. Measurements and computations of flow in pipe bends. J. Fluid Mech., 43: 771-783.

Saysroy, A. and S. Eiamsa-ard, 2017. Enhancing convective heat transfer in laminar and turbulent flow regions using multi-channel twisted tape inserts. Intl. J. Therm. Sci., 121: 55-74.

Sudo, K., M. Sumida and H. Hibara, 2000. Experimental investigation on turbulent flow through a circular-sectioned 1800 bend. Exp. Fluids, 28: 51-57.